Merger and alignment in a reduced model for three-dimensional quasigeostrophic ellipsoidal vortices

Neil Martinsen-Burrell[a)]
Department of Mathematics, University of North Carolina, Chapel Hill, North Carolina 27599

Keith Julien
Department of Applied Mathematics, University of Colorado, Boulder, Colorado 80309

Mark R. Petersen
Computational and Computer Science Division, Los Alamos National Laboratory, Los Alamos, New Mexico 87545

Jeffrey B. Weiss
Program in Atmospheric and Oceanic Sciences, University of Colorado, Boulder, Colorado 80309

(Received 9 February 2006; accepted 3 March 2006; published online 2 May 2006)

We investigate the interaction of two ellipsoidal vortices in the three-dimensional quasigeostrophic fluid equations by first studying a reduced model of vortex interaction, the ellipsoidal moment model, and second by comparing the results to corresponding numerical simulations. The ellipsoidal moment model approximates the interaction of two ellipsoidal lumps of potential vorticity by a finite-degree-of-freedom Hamiltonian system. This approximation is derived explicitly in the natural moment coordinate system to first order in the ratio of the size of the vortices to their separation. Using this Hamiltonian system for the case of initially spheroidal identical vortices, the linear stability of vertically aligned vortices is analyzed. A new dynamical criterion for vortex merger and alignment is proposed and shown to give a clear and reasonable boundary for vortex merger. A similar boundary is shown to exist in the size of the largest Lyapunov exponent, although not in the chaotic region as measured by the 0-1 test of Gottwald and Melbourne [Proc. R. Soc. London, Ser. A **460**, 603 (2004)]. There is no such sharp boundary for vortex alignment in this reduced model. A series of numerical experiments confirms the accuracy of the merger criterion used in the ellipsoidal moment model. The numerical simulations also suggest a mechanism for understanding the process of vortex alignment in terms of vortex Rossby waves. © *2006 American Institute of Physics*. [DOI: 10.1063/1.2191887]

I. INTRODUCTION

The quasigeostrophic (QG) equations approximately describe large-scale motions of the atmosphere and ocean. It is now well known that QG turbulence is dominated by the motion of coherent regions of large potential vorticity (*vortices*) in both two[1–4] and three[5–9] dimensions. The dominance of such relatively simple coherent structures suggests that these systems may be well described by much simpler models. In two dimensions, the dynamics of coherent vortices have inspired many low-degree-of-freedom models. Kida[10] first studied the motion of a single ellipse in a prescribed shear flow, showing that an initially elliptical vortex remained elliptical for all time. Melander *et al.*[11] then modeled the interaction of two ellipses using this model, under the assumption that the vortices were well separated. Using that elliptical moment model to define a critical distance for vortex merger, Weiss and McWilliams[12] gave a simple model of two-dimensional turbulence that agreed well with simulations.

Following a similar course in three-dimensional (3D) QG fluids, moment models were used to study single ellipsoidal vortices in shear flows.[13,14] Miyazaki *et al.*[15] extended these methods to study the interaction of two ellipsoidal vortices. They focused on tall vortices, while QG simulations indicate that most vortices have an aspect ratio (in scaled coordinates) slightly less than 1.[6,7,16] Further, their criteria for merger gave the surprising result that vortices with small vertical separation had radically different critical merger distances than did vortices with no vertical separation. In this paper we will present an alternative way of analyzing merger in the ellipsoidal moment model that is free of this shortcoming. In addition to previous work on moment models in three dimensions, some work has been done on the merger of three dimensional vortices[17–19] using quasigeostrophic simulations although none of them address the question of vortex alignment. The simulations presented here explore the parameter regime where alignment is likely.

Dritschel, Reinaud, and McKiver[20] propose a different ellipsoidal vortex model that is not based on moments. That model has been used to analyze the critical distance for merger of two vortices[21] of various shapes. The technique used there to diagnose vortex merger is one of linear instability of the vortex to ellipsoidal perturbations. They consider the marginal stability curve to be an accurate predictor of the presence of a vortex merger. While that approach is

[a)]Electronic mail: nmb@unc.edu

similar to the one presented here, the two ellipsoidal vortex models are quite distinct and there is no obvious connection between the linear stability criteria and the dynamic criterion described in Sec. III B.

Simulations show that, in addition to merging, three-dimensional QG vortices align vertically, eventually forming tall columns.[7,22] The geometric criteria used by Miyazaki *et al.* cannot address the process of vortex alignment since it considers two vortices with initially small horizontal separation to already be aligned. The dynamic criterion proposed here applies to the evolution of vortices that are initially close to alignment. Using this criterion for vortices that are initially close to alignment shows that, in contrast to vortex merger, there is not a sharp boundary between initial conditions that align and those that do not align.

We also consider quantitatively the chaotic behavior of interacting vortices. While chaos has been observed in the dynamics of three-dimensional QG vortices,[14,15] to our knowledge, this work is the first systematic study of the conditions for chaotic trajectories in the ellipsoidal moment model. We also show here that chaotic trajectories with large positive Lyapunov exponents only occur where a vortex merger is predicted to occur. For this reason we suggest that large Lyapunov exponents in this moment model can be used to identify a vortex merger for three-dimensional vortices.

Finally, in a series of numerical simulations, we confirm the accuracy of the dynamic merger criterion in the ellipsoidal moment model by analyzing merger and alignment in the full 3D QG equations. New quantitative measures of vortex merger and alignment are proposed and used to show that the predictions of the ellipsoidal moment model for the presence of an inviscid vortex merger are accurate. In addition, these simulations suggest that vortex Rossby waves[23,24] may provide a mechanism for the process of vortex alignment.

In Sec. II we will introduce the ellipsoidal moment model, which results from applying the general process of Hamiltonian moment reduction[14] to the three-dimensional QG equations. In Sec. III we will motivate and describe a particular set of simulations carried out using that model. Finally in Sec. IV we will present the results of a corresponding set of numerical simulations of the three-dimensional QG equations.

II. THE ELLIPSOIDAL MOMENT MODEL

The QG equations

$$D_t q = \partial_t q + [\psi, q] = \mathcal{D}, \tag{1a}$$

$$q = -\nabla^2 \psi = -(\partial_x^2 + \partial_y^2 + \partial_z^2)\psi, \tag{1b}$$

where $[f,g]=\partial_x f \partial_y g - \partial_y f \partial_x g$ is the horizontal Jacobian and $\mathcal{D}$ represents any dissipation or forcing, are the equations of motion for a uniformly stratified rotating fluid with unit stratification (for a derivation, see books by Pedlosky[25] and Salmon[26]). The quantity q is called the *potential vorticity* and ψ is a streamfunction for the flow. The fluid velocity $\boldsymbol{u}=(\partial_y\psi, -\partial_x\psi, 0)$ is purely horizontal, so that the fluid moves in layers with vertical coupling coming only from the three-dimensional Laplacian in Eq. (1b). With $\mathcal{D}=0$, these equations are an infinite-dimensional Hamiltonian system[26] with the energy

$$H = -\frac{1}{2}\int_{\mathbb{R}^3} q\psi \, \mathrm{d}\boldsymbol{x}$$

as the Hamiltonian.

The process of Hamiltonian moment reduction[14] is a general process for constructing finite-dimensional Hamiltonian systems from infinite-dimensional ones under certain conditions. The importance of this process is that it allows the development of simple models in a systematic way that preserves important physical and mathematical structure (in this case the conservation of energy and circulation). In addition, the process of moment reduction is relatively systematic compared to the first reduced models of vortex interaction that were complicated to derive and were not explicitly conservative.[13] We apply this process here to the QG equations. The resulting Hamiltonian is, apart from changes in notation, exactly the Hamiltonian of Miyazaki and collaborators.[15,27] We present the reduction in some detail in the Appendix because previous work neither shows the derivation explicitly, nor provides the order of the approximation.

For N disjoint regions of nonzero potential vorticity, the resulting dynamical system is

$$\frac{\mathrm{d}\boldsymbol{b}_i}{\mathrm{d}t} = \tilde{J}\nabla_{\boldsymbol{b}}\tilde{H}, \tag{2}$$

$$H \cong \tilde{H} = \sum_{i=1}^{N} H^{(s)}(\boldsymbol{b}_i) + \sum_{\substack{i,j=1 \\ i<j}}^{N} H^{(p)}(\boldsymbol{b}_i, \boldsymbol{b}_j) \tag{3}$$

with $H^{(s)}$ and $H^{(p)}$ given by Eqs. (A5) and (A7), respectively. The coordinates for each region are $\boldsymbol{b}_i=(a_i^{\boldsymbol{0}}, \boldsymbol{x}_i, c_i^{\boldsymbol{\mu}})$ where $a_i^{\boldsymbol{0}}$ is the total vorticity in the region, $\boldsymbol{x}_i$ is the centroid of the region, and $c_i^{\boldsymbol{\mu}}$ are the second-order central moments of the region.

This is the Hamiltonian of Miyazaki and collaborators.[15,27] In the work of Kida,[10] Meacham[28] and Meacham *et al.*[13] on the behavior of single vortices in linear shear flows, the approximation made here in terms of vortex separation is exact. (One can imagine a linear shear being induced by a vortex at an infinite distance.) Here, for interacting vortices, the error in our approximation is determined by the degree to which the flow induced by an ellipsoid at a finite distance differs from a linear shear.

In two dimensions, this first-order approximation in vortex separation produces a model that is highly predictive of the behavior of vortices in the full fluid equations, even in situations where the vortex separation is comparable to the vortex radius.[12] We proceed with the analogous approximation in three dimensions in the hope that similar accuracy will result. The accuracy of this approximation in predicting the behavior of vortices that are close together can only be verified by comparing the results of the moment model with results from the full QG equations.

We will not use the Casimir invariants for this Poisson bracket nor the conserved quantities resulting from symme-

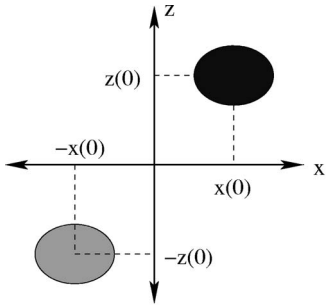

FIG. 1. Schematic diagram of the initial positions of the two vortices and the coordinate system used.

tries of the Hamiltonian to explicitly reduce the dimensionality of our system or work in different coordinates. The physical interpretations of the circulation, the centers of vorticity, and the second-order moments are simple enough and our analysis will not depend on a canonical Hamiltonian structure. These symmetries do determine the dimension of the phase space in which motion occurs. For N vortices, there are $10N$ moments up to second order (see the Appendix). For each vortex, there are four Casimir invariants, allowing a reduction to $6N$ dimensions. The rotational and translational symmetries of the Hamiltonian yield three additional Noether invariants, only two of which are independent, allowing a reduction by four dimensions. Taking into account the conserved energy, motion takes place on a $(6N-5)$-dimensional constant energy surface embedded in a $(6N-4)$-dimensional phase space. Note that for $N=2$, this is an eight-dimensional phase space. We will also use symmetries of the equations of motion to limit the range of initial conditions that we need to investigate. Without loss of generality, we will constrain vortex 1 to be in the first quadrant of the xz plane with volume $4\pi/3$ and circulation $a_1^0=1$, and further constrain the center of vorticity of the two vortices to be at the origin.

III. MOMENT MODEL SIMULATIONS AND RESULTS

In the interest of simplicity, we will only consider here the case of symmetric vortex interaction. In two dimensions, the essence of vortex merger is captured by studying symmetric vortex interactions,[29] although nonsymmetric merger does have many interesting details.[30] For the initial vortex shape, we choose a spheroid whose vertical size is 80% of its horizontal size (in scaled coordinates). This aspect ratio of 0.8 is seen to be the mean vertical aspect ratio of coherent vortices in recent QG turbulence simulations.[7,16] Subject to our constraint that the volume of vortex 1 be $4\pi/3$, which implies that $\alpha_1\beta_1\gamma_1=1$, the initial semi-axes of our vortices are $\alpha_1=\beta_1=\sqrt[3]{10/8}$ and $\gamma_1=8\alpha_1/10$. Fixing $y_1(0)=0$, the remaining initial conditions to be specified are the position of the center of the first vortex: $(x_1(0),z_1(0))\in[0,\infty)\times[0,\infty)$ (see Fig. 1).

Note that it is possible to specify initial positions for the vortex moment coordinates that represent two overlapping vortices in the QG equations. These initial conditions are unphysical and violate our assumption of distinct well-separated vortices, but they are valid initial conditions for the ellipsoidal moment model. Because we are interested partly in studying that model itself, we will not exclude these initial conditions *a priori*.

Trajectories were computed using an adaptive eighth-order Runge-Kutta method from the RKSUITE package.[31] An elliptic integral must be computed to calculate the phase-space gradient of the self-energy $H_i^{(s)}$. This is done using an adaptive subroutine of QUADPACK.[32] While we do not use an integrator that enforces symmetry or conservation quantities, these conditions are all maintained with a maximum error of 10^{-12}. Some examples of the paths taken by one of the two vortices are shown in Fig. 2 for two different initial positions. In addition to computing single trajectories, we also computed the largest positive Lyapunov exponent for each trajectory using a rescaling method.[33,34]

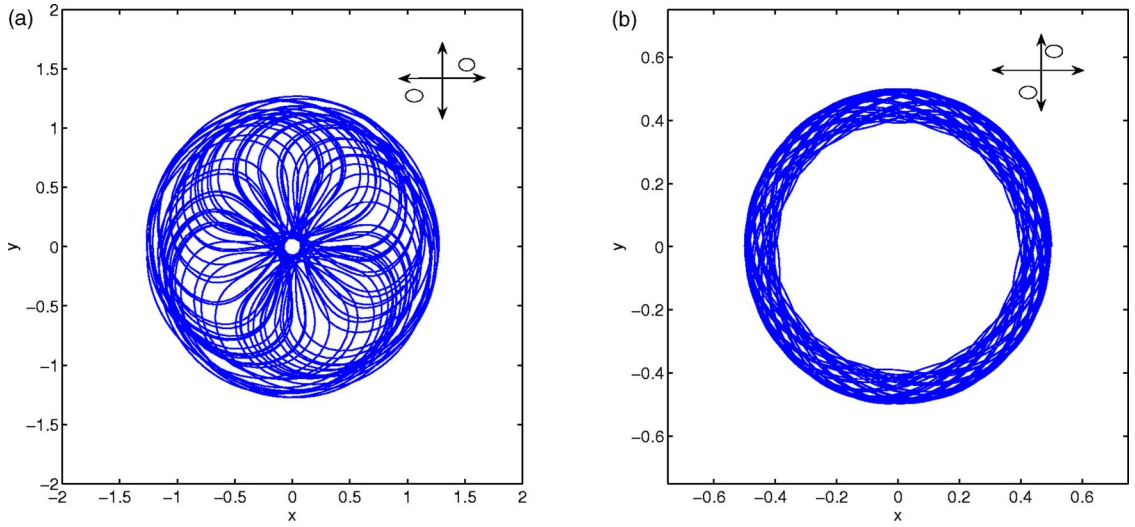

FIG. 2. Trajectories projected into the xy plane for vortices with initial positions (a) $x_1(0)=1.275$, $z_1(0)=0.175$ and (b) $x_1(0)=0.5$, $z_1(0)=1.0$ as shown schematically in the insets.

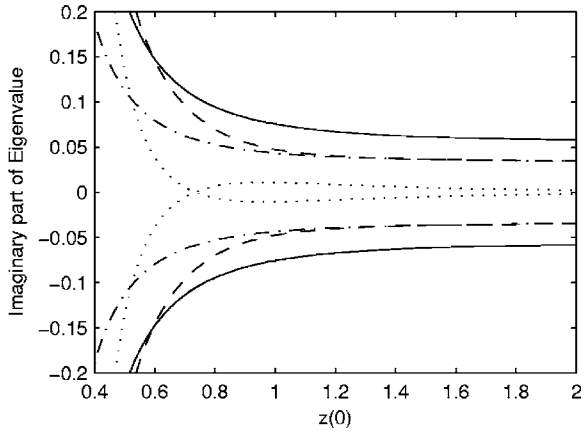

FIG. 3. The imaginary parts of the nonzero eigenvalues for the vertically aligned fixed points vs $z_1(0)$. The different line styles represent distinct eigenvalue pairs.

As a further measure of chaos, we used a new 0-1 test for chaos developed by Gottwald and Melbourne.[35] The advantages of this method are that it has many less free parameters, it is computationally cheaper because there is no need to compute both a reference and a perturbed trajectory and it gives an unambiguous result for the existence of chaos. The latter is also a weakness of the method, as it cannot distinguish between various "strengths" or time scales of chaos. In a system such as the ellipsoidal moment model with many degrees of freedom, chaotic motion may occur in different ways on different time scales. These different sorts of chaos cannot be distinguished by such a binary test.

A. Linear stability of fixed points

For symmetric vortices with a circular cross section such as we study here, there is a family of fixed points for $x_1(0)=0$ when the two vortices are initially vertically aligned. By numerically computing the stability of these fixed points, we see that they are all elliptic fixed points. The 20-dimensional Jacobian matrix has 10 zero eigenvalues corresponding to eight conserved Casimir invariants and two independent symmetry invariants. The remaining ten eigenvalues have zero real part and occur in five conjugate pairs. Two of these pairs are themselves equal due to the interchangeability of the two vortices.

Of the four distinct eigenvalue pairs, one is distinctive in the following manner. For very large $z_1(0)$, the vortices are essentially decoupled and each vortex independently has two vanishing eigenvalues that are due to the two independent symmetry invariants of the single-vortex Hamiltonian $H^{(s)}$. For finite values of $z_1(0)$, there are only two independent symmetries of the full Hamiltonian rather than two for each vortex. Thus, there are two eigenvalues that diverge from zero at finite separation, which correspond to the broken symmetry of the interacting vortex system [see Fig. 3 for the imaginary parts of the eigenvalues for different values of $z_1(0)$].

This family of elliptic fixed points (and their analog for more than two vortices) controls the behavior of columns of many, nearly aligned vortices. For stacks of as many as 100 vortices, with separations as large as four units and as small as one unit, all of the fixed points of the ellipsoidal moment model are elliptic. The spiral and rotating waves of vortex columns seen in simulations[22] might be explained by the oscillatory linear response of nearly aligned vortices as described here. Another conclusion based on these linear results is that tall stacks of ellipsoidal vortices are not unstable to small perturbations of the vortices. This is in direct contrast to the stability of tall vortex columns.[36]

B. Merger/alignment diagnostics

An important physical question that can be addressed using the ellipsoidal moment model is when two QG vortices merge. Such investigations have been carried out in two dimensions[37] and compare favorably with numerical simulations[30] and experiments.[38] In two dimensions, there is little ambiguity in determining when two vortices in the moment model merge: the Hamiltonian becomes singular when their centers of vorticity coincide. In three dimensions, since the centers of vorticity move on horizontal planes, the centers of two vortices will never coincide unless they initially lie on the same horizontal plane. This necessitates the development of diagnostics for merger and alignment that can be applied to moment model trajectories. Miyazaki *et al.*[15] use the criteria that two vortices in the moment model are considered to have merged or aligned when they overlap vertically and their centers are separated by a distance of less than $(\alpha_1\beta_1\gamma_1)^{1/3}+(\alpha_2\beta_2\gamma_2)^{1/3}$, which is the sum of the geometric mean of the semi-axes of the two vortices. While geometrically and intuitively compelling, these criteria for alignment give the surprising result that vortices with small vertical separation have smaller critical horizontal separations for merger than those with larger vertical separations. While a similar trend is seen by Reinaud and Dritschel[19] in an analysis of merger using contour dynamics simulations, it is not nearly as extreme as that predicted by Miyazaki *et al.* In addition, these criteria do not allow for the study of further alignment of vortices that initially satisfy this criteria nor does it allow for the alignment of vortices that do not overlap vertically, which is commonly seen in simulations.[6,22]

As opposed to the physical criterion of overlapping vortices, we propose a dynamic geometric criterion based on the behavior of trajectories of the ellipsoidal moment model. Consider the horizontal separation $r_h(t)=2\sqrt{x_1(t)^2+y_1(t)^2}$ between the centers of vorticity of the two vortices. Intuitively, in the full QG equations, this quantity goes to zero for vortices that merge or align fully. Due to dissipation in the full system, merger and alignment appear to be irreversible processes. On the other hand, in the conservative moment model, vortices may approach very close to one another and then move apart [see Fig. 2(b)]. To account for the possibly large variation in r_h, we examine the minimum value that it attains over the length of the simulation. We plot $\mathcal{R}=\min_t r_h(t)/r_h(0)$ for a range of initial positions in Fig. 4.

The transition between merger and nonmerger is clear along the x_1 axis. The sharp transition persists for increasing vertical separations up to approximately $z_1=0.95$. For larger vertical separations, there is no longer such a sharp transition

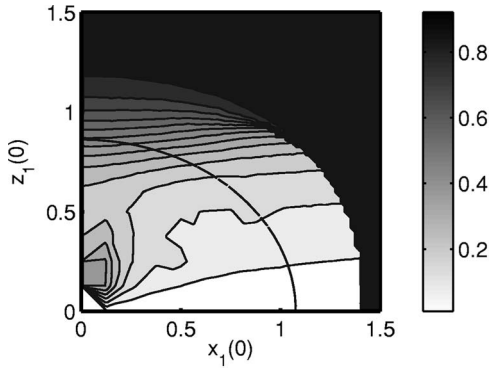

FIG. 4. Contours of $\mathcal{R}=\min_t r_h(t)/r_h(0)$ for varying initial positions $[x_1(0),z_1(0)]$. The solid line is the curve of initial positions that result in two vortices that are initially touching.

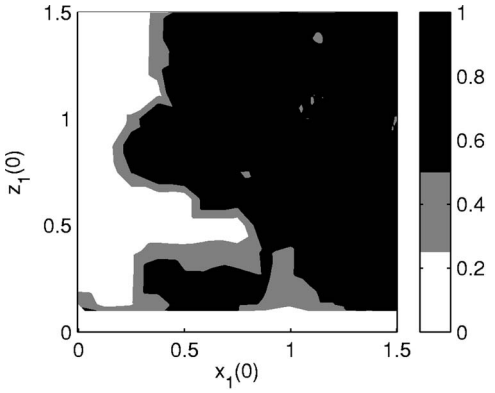

FIG. 6. The Gottwald-Melbourne statistic vs initial position. Values close to 1 indicate the presence of chaos. The heavy contour is at a threshold of 0.5.

between merging and nonmerging initial conditions. In particular, near the z_1 axis, we see a smooth transition with decreasing z_1 from values of $\mathcal{R}$ near 1 to small values of $\mathcal{R}$. This is the region where we would expect to see evidence of vortex alignment in this model. From these data we conclude that vortex merger and alignment are two distinct processes, with a sharp transition between merger and nonmerger, but a smooth transition between alignment and nonalignment. Finally, although there is structure in the nonphysical region where the vortices initially overlap, this cannot be inferred to have any implications for the behavior of overlapping quasigeostrophic vortices.

C. Lyapunov exponents

In addition to this analysis of individual trajectories, we seek to understand the dynamical structure of the system using local measures of chaos. One such measure is the largest positive Lyapunov exponent for a given trajectory (labeled by its initial condition), shown in Fig. 5. Chaos with a large Lyapunov exponent occurs inside the region where merger was determined to occur in Sec. III B. In other regions where the largest Lyapunov exponent is small, we cannot conclude that chaos does not exist (see Sec. III D), only that it does not exist on a comparable time scale to that of the chaotic merger region.

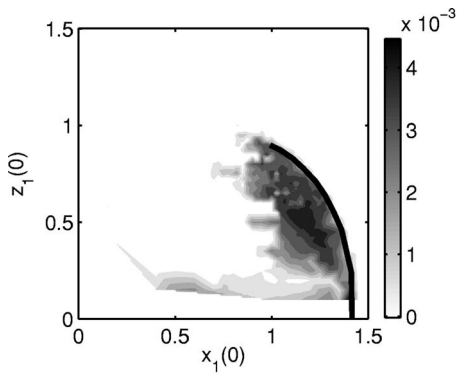

FIG. 5. Largest positive Lyapunov exponent as a function of $[x_1(0),z_1(0)]$. The solid line is the boundary between large and small values of $\mathcal{R}$, as seen in Fig. 4.

A similar correlation between the boundary between chaotic and nonchaotic behavior and the boundary between merger and nonmerger is seen in two dimensions,[12] although the singularity of merging vortices in two dimensions prevents accurate computations of the Lyapunov exponents inside the merger boundary. Another similar correlation between vortex merger and chaotic motion is seen in investigating the merger of point-vortex clouds.[39] The computation of Lyapunov exponents further supports the conclusion of the previous section that vortex merger and vortex alignment are distinct processes, given the lack of large positive Lyapunov exponents for initial conditions near the z_1 axis.

D. 0-1 test for chaos

Another local measure of chaos is the 0-1 test of Gottwald and Melbourne.[35] Using some function of the trajectory as forcing for an auxiliary dynamical system, the motion of the auxiliary system may be examined to determine the presence of chaos in the initial trajectory. In the theoretical case of infinite integration, the method yields 0 if the initial trajectory is not chaotic or 1 if it is. In practice, for finite integration times, intermediate values of the statistic are obtained, but a clear distinction between chaos and nonchaos is still possible as the results for these simulations are quite close to either 0 or 1. In addition, the results are not sensitive to the integration time used as long as it is sufficiently large. The distinct disadvantage of such a binary test for chaos is that it cannot distinguish between chaos on different time scales, as is possible with Lyapunov exponents. In a system such as the ellipsoidal moment model with many degrees of freedom there are many possible sources of chaos with differing characteristic time scales. Contrasting the Lyapunov exponent results of Fig. 5 with the results of the Gottwald-Melbourne statistic in Fig. 6, it is apparent that for some initial conditions with small Lyapunov exponents, there is still chaotic motion present. In fact, the only initial conditions that exhibit regular behavior according to this statistic are those close to the elliptic fixed points of Sec. III A. Near those fixed points, the linear behavior discussed in Sec. III A predicts that contours of $\mathcal{R}$ should be horizontal. Inspecting the contours in Fig. 4, the distance from the $z(0)$ axis at

which they deviate from the horizontal due to the influence of nonlinearity corresponds well to the distance at which the trajectories become chaotic in Fig. 6.

IV. 3D QG SIMULATIONS AND RESULTS

A. The numerical model

The numerical code used to integrate the three-dimensional QG equations (1) is a fully pseudospectral model[40,41] with de-aliasing. For the timestepping, we choose a mixed implicit/explicit third-order Runge-Kutta method that treats the linear dissipation terms in (1a) implicitly, and requires only one additional level of storage.[42] In order for the numerical solutions to remain well behaved, we must choose $\mathcal{D}$ to be nonzero. The traditional choice is some form of diffusion with $\mathcal{D}=\mathcal{D}_p=(-1)^{p+1}\nu_p\nabla^{2p}q$ for $p=1,2,\ldots$. Using this choice with $p=1$ gives ordinary Newtonian viscous dissipation, while higher values of p (referred to as *hyperviscosity*) are often used in turbulence simulations to give lower energy dissipation while still maintaining smoothness at the grid scale. One drawback of using hyperviscosity in simulations focused on individual vortices is that it can radically change the vorticity profile within a vortex. To avoid this we use ordinary viscosity $\mathcal{D}=\mathcal{D}_1$ in our simulations with $\nu_1=1\times10^{-4}$. Making this choice does introduce significant dissipation in our numerical simulations with the energy dropping to 60% of its initial value over the length of the simulations. As a result of this significant dissipation, attention must be paid to differentiating the effects of dissipation from the effects of the inviscid evolution with $\mathcal{D}=0$.

Our problem domain will be a triply periodic box $[-L/2,L/2)^3$ with $n=128$ grid points in each direction. The side length $L=10$ is chosen to be large compared to both the size and separation of the original vortices, so that the vortices are always far away from the edges of the box. This is necessary to minimize the effects of approximating an infinite domain with a periodic box. Tests with a box of twice the size (and twice the resolution) show no qualitative difference. In addition, we do not impose the condition that the net circulation integrated over the domain be zero, which is ordinarily enforced in triply periodic simulations, instead using zero far-field potential vorticity, as in the preceding sections.

We choose initial vorticity distributions that closely match those used in the derivation of the ellipsoidal moment model (Sec. II). Our initial condition consists of two separate regions of nonzero potential vorticity. For simplicity and comparability with the previous moment model calculations, we restrict our attention here to identical vortices. Since the numerical simulations require smooth initial data, it is not possible to replicate exactly the moment model's assumption that each vortex has uniform vorticity in its interior. Instead, the vortices used here will have a smooth potential vorticity profile given by

$$q=\frac{q_0}{2}\{(1+\tanh[10(1-r)]\}=q_0f(r), \tag{4}$$

where $r^2=(x-x_0)^2/c_x^2+(y-y_0)^2/c_y^2+(z-z_0)^2/c_z^2$. The factor 10 is chosen large enough to give each vortex a sharp edge, but not so large as to produce Gibbs phenomena. The peak potential vorticity value q_0 is chosen so that each vortex has unit circulation $q_0\int_{\mathbb{R}^3}f(r)\,dV=1$ (for comparison with the ellipsoidal moment model results), where $f(r)$ is the radial profile specified in Eq. (4).

Fixing the above potential vorticity distribution for each vortex, we are left to choose the initial position of each vortex and the shape of the two vortices as determined by c_x,c_y,c_z. We choose the vortices to be initially spheroidal with $c_x=c_y$. The vertical aspect ratio c_z/c_x is chosen to be 0.8, as in Sec. III. Finally, to fix the size of the vortex, we choose $c_xc_yc_z=1$. In keeping with our previous orientation, we choose the vortices to be centered around the origin with $y_0=0$. Our family of simulations then consist of varying x_0 and z_0 over portions of the first quadrant [see Fig. 7(a) for an example].

B. Quantitative measures of alignment

Quantitative measures of vortex behavior are crucial for analysis of these three dimensional fluid simulations. Visual analysis is a powerful tool for recognizing the results of vortex interactions, but it has limited applicability to collections of many simulations such as those described here. Vortex alignment presents a particularly difficult diagnostic challenge since its effects are not as dramatic as those of vortex merger.

The total circulation

$$\mathcal{Q}=\int_{\mathbb{R}^3}q\,d\boldsymbol{x} \tag{5}$$

and total angular momentum

$$\mathcal{L}=\int_{\mathbb{R}^3}(x^2+y^2)^{1/2}q\,d\boldsymbol{x} \tag{6}$$

are globally conserved quantities of the inviscid QG equations. As such, the progression of time can only result in a rearrangement of the integrands of these two integrals: the potential vorticity and the angular momentum. Motivated by this view of the evolution as one of rearrangement, we propose two measures dealing with the location in the problem domain of a certain fraction of these conserved quantities. Consider

$$Q(r)=\int_{C_r}q\,dV$$

and

$$L(r)=\int_{C_r}(x^2+y^2)^{1/2}q\,dV,$$

where C_r is the vertical cylinder of radius r centered on the origin. These are, respectively, the circulation and angular momentum contained in C_r. From these radial distributions, we can construct median radii $r_Q(t)$ and $r_L(t)$ such that $Q(r_Q)/\mathcal{Q}=L(r_L)/\mathcal{L}=1/2$ at every time t.

The intuition behind these measures is that after merger when the potential vorticity is concentrated in one vortex, r_Q will have decreased because more of the vorticity will be closer to the centerline of the domain, requiring a cylinder

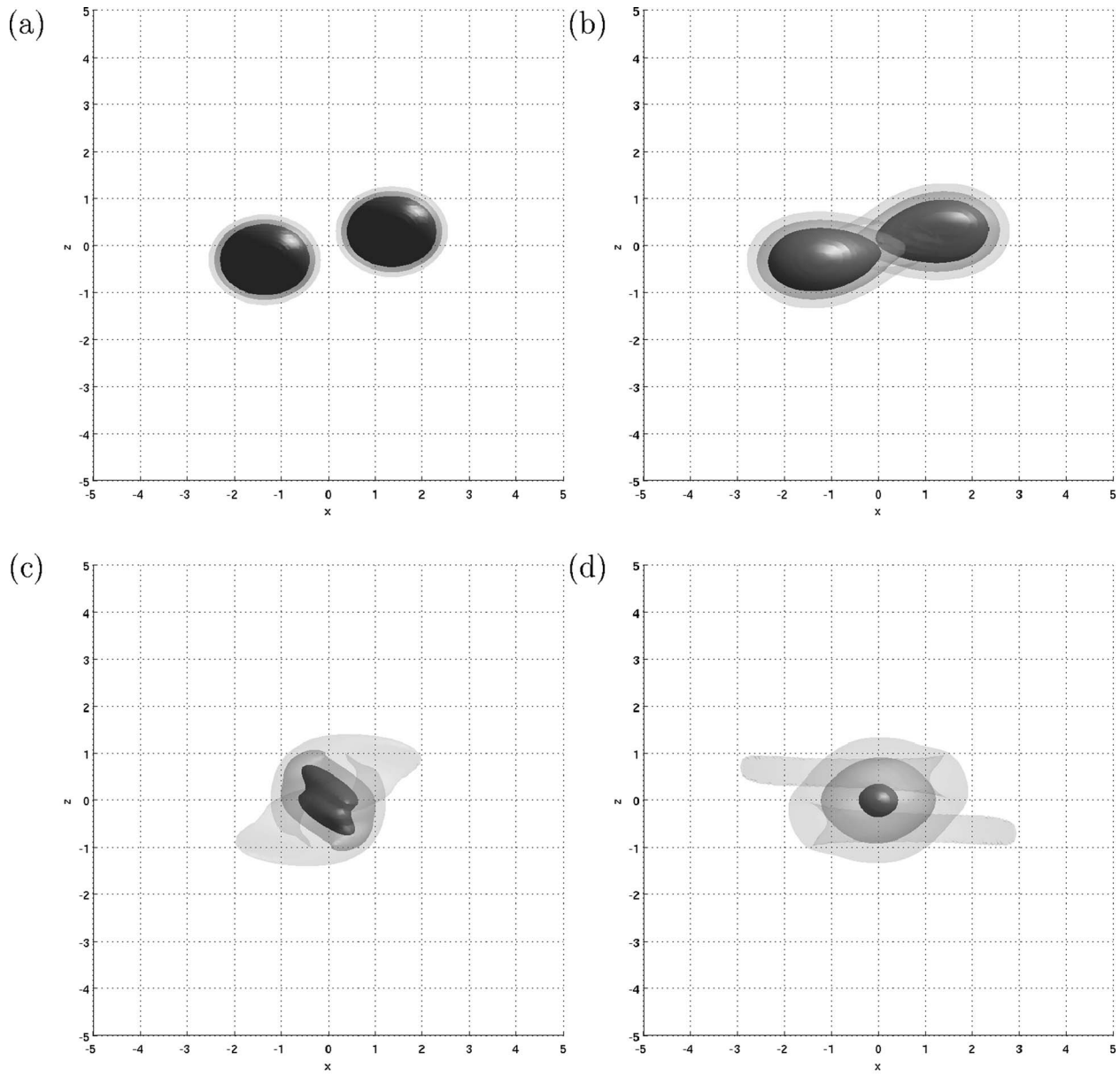

FIG. 7. Snapshots of the evolution with $x_0=1.35$ and $z_0=0.3$ at (a) $t=0$, (b) $t=50$, (c) $t=200$, and (d) $t=500$. The isosurfaces are at 90%, 50%, and 10% of the maximum potential vorticity at that time. The view is looking down the y axis onto the xz plane.

with smaller radius to capture half of the total circulation. Similarly, when the potential vorticity is concentrated near centerline of the domain, r_L must be larger in order to capture half of the angular momentum, since potential vorticity located near the centerline has less angular momentum. Note that alignment is treated on an equal footing with merger in these measures and that they can also be applied to the results of moment model calculations (by constructing a matching discretized potential vorticity field based on the given moments).

A different set of diagnostics exists for comparison with the ellipsoidal moment model; namely, the moments themselves. In order to compute the 20 moments up to second order [cf. Eq. (A3)] it is necessary to identify the regions D_1 and D_2 over which the integrals are defined. In general, for a continuous three-dimensional distribution of potential vorticity, this is a difficult problem of segmenting the field into disjoint regions according to some criteria that matches the intuitive division into coherent structures. A simple approach of dividing the problem domain in half with a plane through the origin (to preserve symmetry) provides good segmentations when the vortices are nearly circular but not when the vortices are greatly deformed. While segmentation followed by computation of moments can provide information about the quantitative relationship between the moment model and 3D QG simulations, it is of limited utility for the study of vortex merger and alignment because of the large distortions in vortex shape that occur during these processes.

C. 3D QG vortex merger results

Vortex merger results from initial vortex positions with small vertical separation between the two vortices and horizontal separation less than some critical value (which in turn

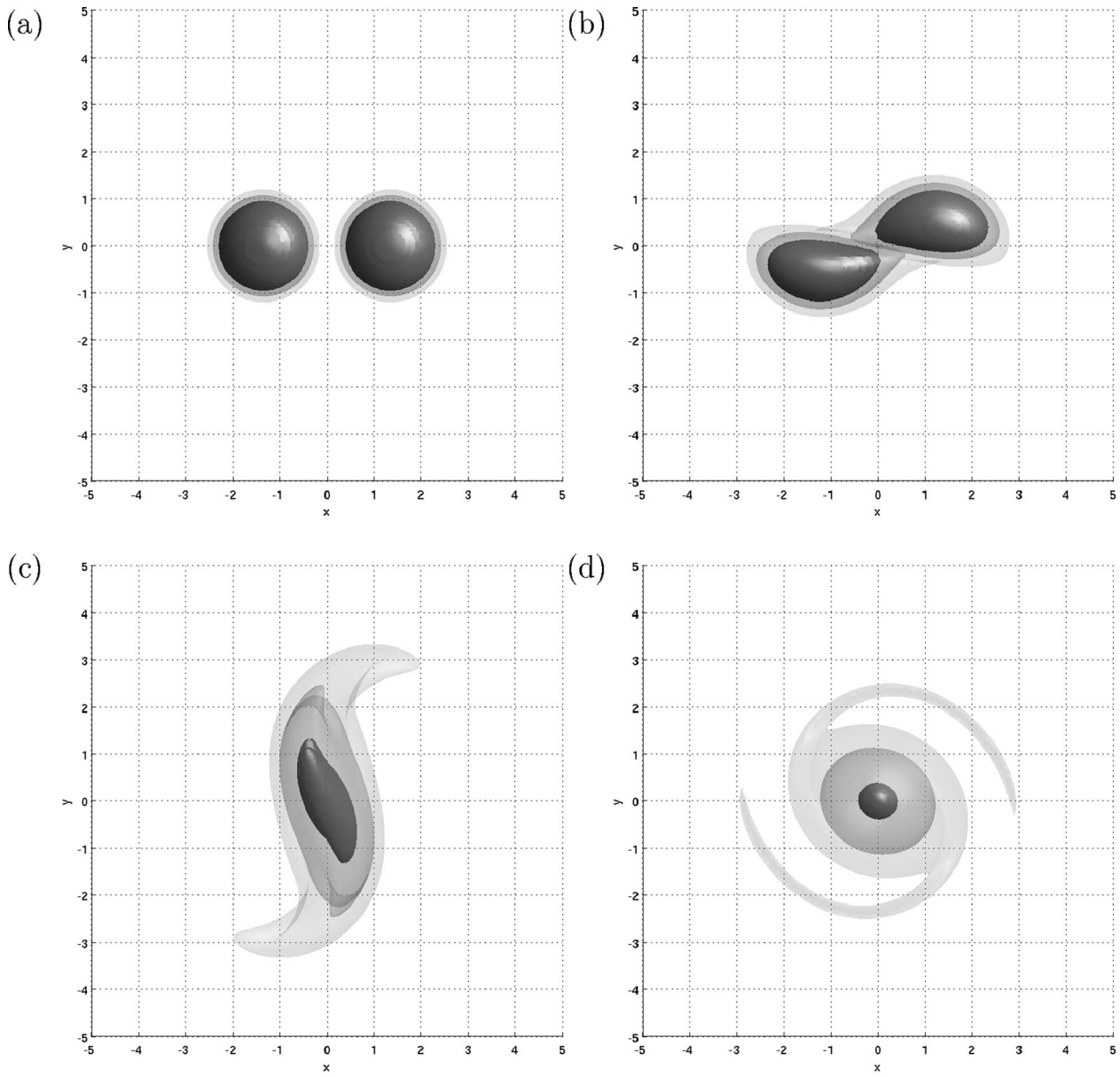

FIG. 8. As in Fig. 7, but with a view down the z axis.

depends on the initial vertical separation). The ellipsoidal moment model provides a prediction of the range of initial vortex positions where merger will occur (cf. Fig. 4). These three-dimensional simulations confirm the predictions of that model. Figures 7 and 8 show snapshots of the evolution of a representative vortex merger with a small vertical offset. As seen there, each vortex develops a fast-moving "handle" that moves in towards the other vortex. The remaining bulk of the vortex develops filamentary structures [see especially Figs. 8(c) and 8(d)]. These filaments are rapidly dissipated leaving only one vortex by $t=500$. Total dissipation in this simulation is not too severe, with the maximum value of the potential vorticity falling to 93% of its initial value by $t=500$. The merger does produce a significant re-arrangement of vorticity, with the final vortex being substantially more diffuse than either of the two original vortices. The process seen here is similar to that described by[17] for vortices with initially smoother profiles. With the lower dissipation used in those experiments, the filaments are longer lived than those seen here.

Merger boundary

To illustrate the utility of the merger statistics that we developed in Sec. IV B we see in Fig. 9(a) that $r_Q(t)$ decreases to approximately 70% of its initial value during the merger process for the simulation shown above. This validates our intuition that r_Q should decrease as the vortices merge and the bulk of the potential vorticity moves closer to the z axis. The increase of r_Q after $t=450$ is attributed to diffusion acting on the resulting merged vortex. Similarly, as expected [Fig. 9(b)], r_L increases when the vortices are merging, as the angular momentum contained in a cylinder of fixed radius decreases due to the inward movement of poten-

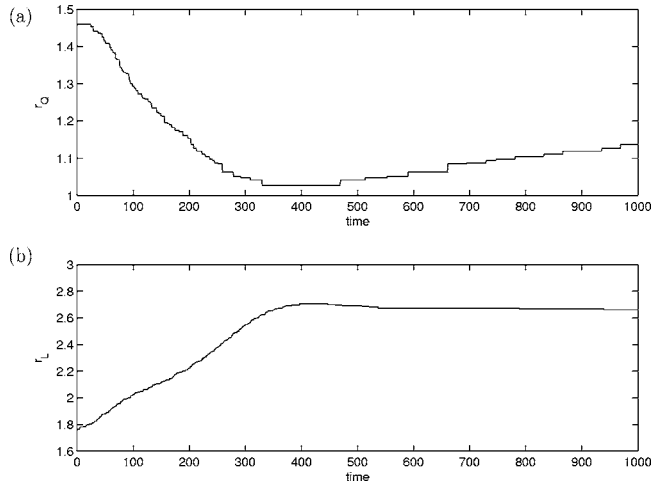

FIG. 9. Time series of (a) r_Q and (b) r_L for the simulation shown in Figs. 7 and 8. The discreteness apparent in (a) is due to the resolution of the grid.

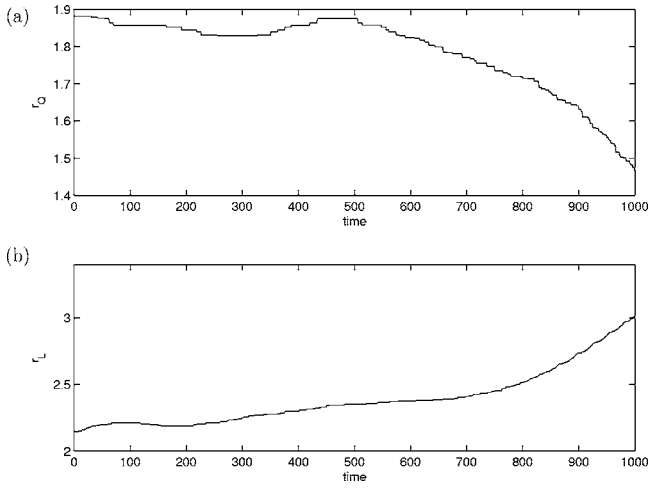

FIG. 11. Time series of (a) $r_Q(t)$ and (b) $r_L(t)$ for $x_0=1.8$ and $z_0=0$.

tial vorticity. Thus, to contain half of the total angular momentum requires an increase in r_L. The maximum increase of r_L is 54% over the course of the merger.

Having established that r_Q and r_L provide clear evidence of vortex merger, we can use those diagnostics on a range of simulations to distinguish the region where vortex merger occurs. Figure 10 shows the minimum of $r_Q(t)/r_Q(0)$ over the length of the simulations (1000 time units). Merger clearly is occurring in a region similar to that predicted by the ellipsoidal moment model (compare especially Fig. 5), although relatively small minimum values of r_Q are observed for initial conditions with horizontal separations as large as $x_0=1.8$, the largest value simulated. In contrast to the moment model, in these simulations we must contend with the effects of dissipation. The dissipation operator $\mathcal{D}$ causes individual vortices to spread out and become wider. Since the critical merger distance is in terms of the ratio of separation to size, spreading brings vortices "closer" in this sense. Thus it is possible for vortices that do not begin merging at the initial time to diffuse and then merge at a later time. Looking at the evolution of r_Q over time for such an example (Fig. 11), we see that the decrease in r_Q to its minimum value does not begin until relatively late in the simulation, especially compared to the simulation shown in Fig. 9, which has essentially completed the merger process by $t=500$.

We wish to somehow discriminate between those initial conditions in which the vortices eventually merge as a result of diffusive spreading and those where the vortices merge immediately because the initial condition is inside the merger region. To so discriminate, we contour in Fig. 12 the time at which the minimum value of r_Q occurs ($t_{\min}$) such that $r_Q(t_{\min})=\min_t r_Q(t)$. Heuristically, we can say that minima that occur at early times are due to the immediate merging of vortices while those that occur later are due to the diffusive spreading of vortices leading to eventual merger. Quantitatively, define a threshold value of $t_{\min}$ where we say that minima that occur at times later than the threshold were not due to initial conditions in the merger region, but were instead products of the spreading of the two vortices under the action of diffusion. Arbitrarily choosing a threshold time of $t=500$ and a threshold of 80% for the decrease in $r_Q(t)$ gives us the merger boundary shown by the solid line in Fig. 13. Similarly, we can use r_L and the time at which it attains its

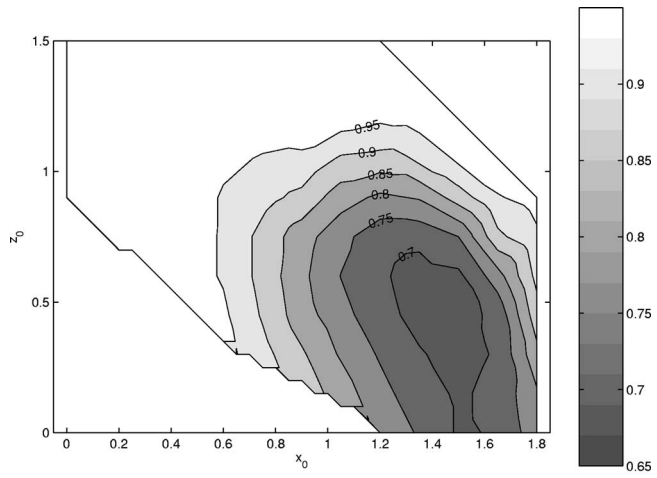

FIG. 10. Contour plot of $\min_t r_Q(t)/r_Q(0)$ vs (x_0,z_0).

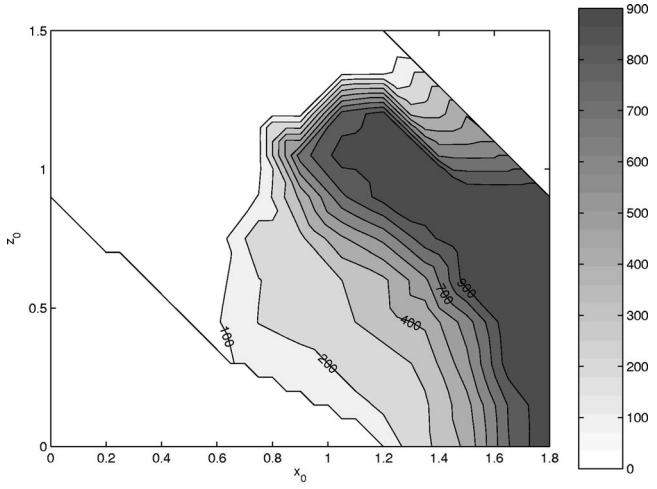

FIG. 12. Time at which the minimum of $r_Q(t)/r_Q(0)$ occurred vs (x_0,z_0).

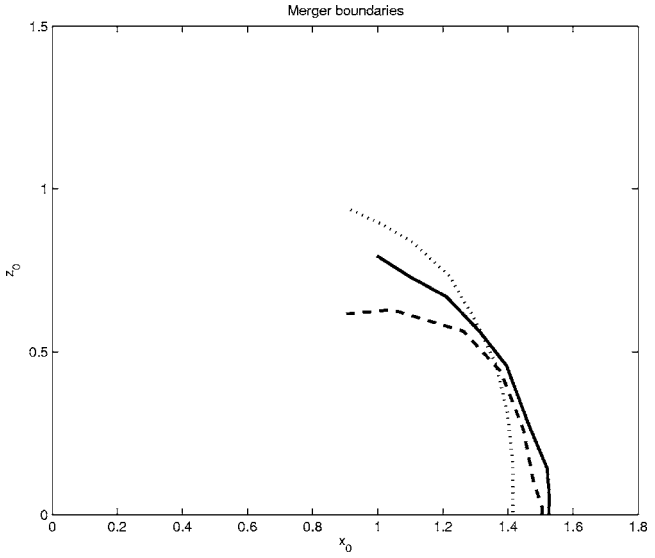

FIG. 13. Merger boundary computed using r_Q (solid) and r_L (dashed) with threshold times of $t=500$. The dotted line is the merger boundary predicted by the ellipsoidal moment model (cf. Fig. 4).

maximum value to also identify initial conditions that lie within the merger region. The boundary determined using the same threshold time and requiring that r_L increase by 40% gives the dashed line in Fig. 13. This choice of the threshold time over which to consider the action of diffusion as irrelevant is reasonable in that a clear merger event shown in Figs. 7 and 8 is complete within 500 time units. Additionally, the threshold time is close to the diffusion time scale set by the size of the vortices $\tau_{\text{diff}}=L^2/\nu_1=(2/10)^2/(1\times10^{-4})=400$ over which we would expect the effects of diffusive transport to be important. To reinforce our choice of threshold values, computing r_Q and r_L for the moment model calculations produces a merger boundary at the 80% threshold that is indistinguishable from that shown by the dotted line in Fig. 4.

D. 3D QG vortex alignment

Simulations of two vortices initially in the alignment region confirm the predictions of the ellipsoidal moment model as to the distinction between the alignment and merger regions. Measurements of the median radii for circulation and angular momentum do not show the dramatic variations seen in merger simulations, nor is there a clear change in qualitative behavior that would identify an alignment region. Looking at Fig. 10, we can see that r_Q does not change by more than 5% for many of the initial conditions in the alignment region (white regions) compared to a 35% change for initial conditions in the heart of the merger region (gray regions). Using data segmentation to compute moments confirms the absence of any dramatic effects of decreasing initial separation on the evolution of two vortices with large vertical separation. In fact, significant alignment of two vortices similar to these is *not* observed in our simulations. In an inviscid model such as the moment model, vortices do not align (or merge) permanently but instead have highly recurrent dynamics (see Fig. 2). Thus, the absence of alignment in our simulations is not in conflict with the results of Sec. III B, which show only a moderate variation in horizontal separation r_h for vortices in the alignment region. Rather, the distinctions between the two models suggest that alignment is neither an inviscid process nor due solely to the addition of viscosity. The observed phenomenon of alignment in turbulence simulations[17] might be due to the much longer time scales there, whereby some process of gradual equilibration in the presence of a fluctuating background could result in alignment.

To learn more about the inviscid behavior of vortices in the alignment region, we need to investigate the three-dimensional structure of the vortices as they align. Figure 14 shows the evolution of two vortices with $(x_0,z_0)=(0.6,0.9)$ at various times in a high-resolution simulation with $n=256$ spectral modes in each direction (and $\nu_1=1.25\times10^{-5}$). There appears to be a traveling wave-like structure that moves up and possibly back down the vortex before its motion is damped out. The wave motion also appears in the evolution of the separation of the two vortices' centers. These waves appear to be part of an adjustment in vortex shape that leads to a relative equilibrium configuration which persists for the remainder of the simulation. These vortex waves are seen in most of the simulations in the alignment regime, although not necessarily as dramatically as illustrated here. Note that these waves are unconnected to the rotational oscillations predicted by the ellipsoidal moment model and that they are not caused by diffusion.

The traveling waves seen here appear similar to those found by Schechter, Reasor, and Montgomery[43] to be responsible for the alignment of a QG vortex column. Their approach is to consider a background state consisting of a vertically aligned vortex column with a smooth radial potential vorticity profile. Superimposed on this background state they consider a perturbation which results in a tilted vortex. This perturbation is then decomposed into a superposition of waves supported by the background state, called *vortex Rossby waves*.[24] These waves damp by resonant interactions with the background state, resulting in an aligned vortex. It is possible that a similar process is occurring in the two vortex situation presented here. The two-vortex configuration could be decomposed into a suitable background state (possibly a steadily rotating V-state[19]) and a perturbation. If the background state supports waves and these waves are damped by resonant interaction with the background, then this might provide an explanation for the adjustment process seen in Fig. 14. This connection with vortex Rossby waves is still quite preliminary and appears difficult to proceed further with; first a suitable background state must be identified, then its linear eigenfunctions must be analyzed and finally the resonant damping of those waves must be examined. All of these steps are complicated by the fully three-dimensional background state and might be resolvable only numerically (and possibly not even then).

Based on these results we propose the following mechanism for vortex alignment in QG turbulence. A pair of vortices which is, for some reason, brought into a marginally aligned state is subject to nearly random perturbations from the other, distant vortices. These perturbations excite vortex

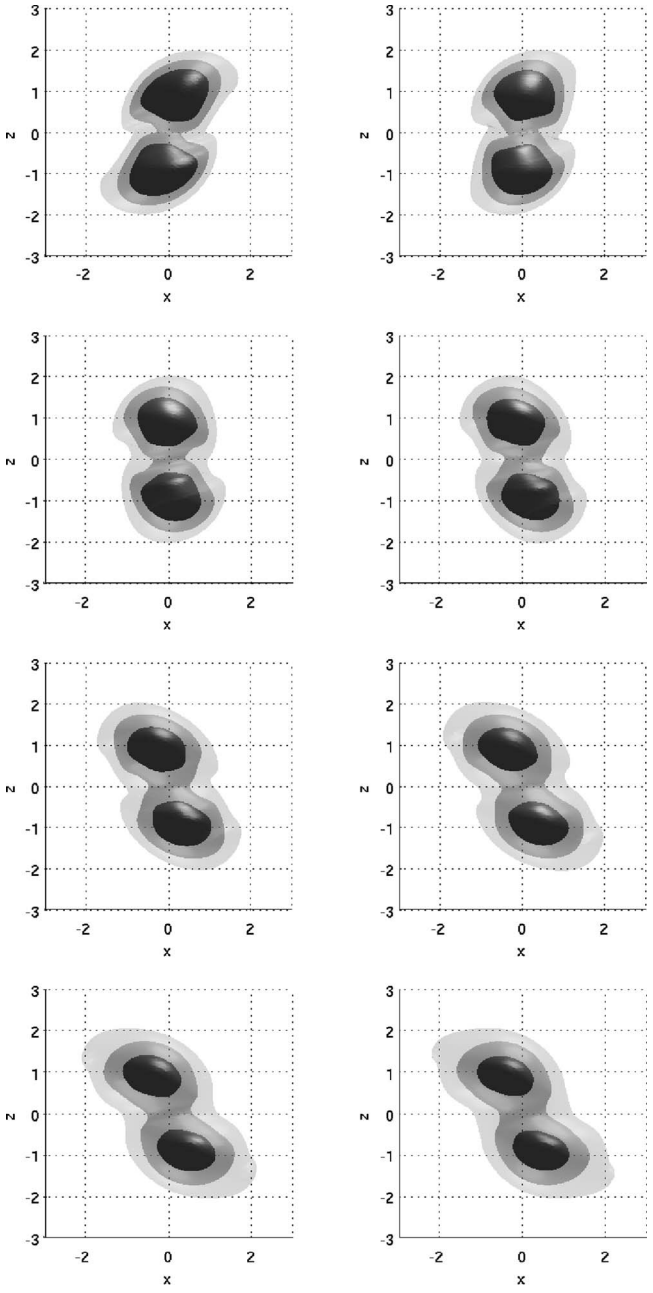

FIG. 14. Evolution of the $q=0.2$ isosurface for two vortices with $(x_0,z_0)=(0.6,0.9)$. The shading is proportional to the local curvature of the surface in order to highlight the structure of the surface. Time advances to the right and downwards; $t=150$ in the first frame and successive frames advance by 25 time units.

Rossby waves which damp resonantly, amplifying the background state. The emission of Rossby waves serves as an adjustment process, in that resonant damping of emitted waves preferentially drives the vortices to a more aligned state. The strong alignment seen in QG turbulence arises after many such perturbation and wave-emission events. We note that this proposed mechanism is, at present, merely a conjecture, and much work remains to demonstrate whether it is, in fact, the reason for vortex alignment in QG turbulence.

V. CONCLUSION

In this work, we have investigated the merger and alignment of interacting quasigeostrophic vortices using the ellipsoidal moment model and confirmed the results with corresponding numerical simulations. After explicitly deriving a finite-dimensional Hamiltonian system in a natural coordinate system as an approximation to first order in the separation of the vortices, we have studied the presence of chaos in this system. The only regular regions in the symmetric vortex case are near the family of stable fixed points that are present for vertically aligned circular vortices. Away from these fixed points, a 0-1 test for chaos shows that all trajectories are chaotic. Lyapunov exponent analysis shows that large positive exponents only exist in regions where we can expect the two vortices to merge. The initial conditions where we might expect vortex alignment to occur do not have large positive Lyapunov exponents. Thus it is proposed that the presence of a large positive Lyapunov exponent for a trajectory of the ellipsoidal moment model can be used as a simple test for the merger of two vortices in the full QG equations.

A family of three-dimensional simulations of the QG equations are performed to verify the conclusions of the ellipsoidal moment model with respect to vortex alignment and merger. New quantitative measures of vortex behavior are proposed and used to determine a boundary for inviscid vortex merger. The boundary as determined is very close to that found using the ellipsoidal moment model. These simulations should be considered as validating the results of Sec. II for vortex merger. In addition, the results presented here validate the conjecture of Reinaud and Dritschel[19] that the critical merger distance for vortices of this aspect ratio should be monotonic in the vertical separation. For unit-aspect-ratio vortices, Reinaud and Dritschel[19] have computed a boundary for merger exactly as shown in Fig. 13 and the qualitative agreement with the boundary computed here is quite good. In a subsequent investigation of the critical distance for merger using stability techniques,[21] those authors compute a boundary for merger with respect to many more parameters than we do here. While this makes it difficult to compare the results directly, their critical merger distance for nearly horizontally aligned vortices is 2.7 compared with our result of 2.8.

The ellipsoidal moment model is not asymptotically valid in the region where vortex merger is predicted to occur, but it still has significant predictive value, especially in the case of vortex merger as shown here. Dissipation plays a role in initiating merger events in these simulations as it spreads individual vortices and thus brings them relatively closer together. The effects of dissipation can be separated from the inviscid dynamics based mainly on the time scale over which they occur. Such separation requires setting time thresholds that can give quantitatively different results, but the qualitative features of the region where vortex merger occurs are insensitive to the particular threshold times chosen. Vortex alignment is seen to be a much more ephemeral phenomenon than vortex merger. In particular, for initial conditions that are already substantially aligned, there is little change in the median radii for circulation or angular momentum. This also

confirms the predictions of the ellipsoidal moment model, which clearly shows a distinction between alignment and merger. A more detailed look at the three-dimensional structure of vortices in the alignment region shows wave-like oscillations of the vortex surface that are not accounted for by the ellipsoidal moment model. This leads us to suggest vortex Rossby waves as a possible explanation for this evolution.

The ellipsoidal moment model provides an example of a high-dimensional Hamiltonian system with clear physical interest and sophisticated dynamics. We suggest that this system of equations is worthy of further study in the context of dynamical systems. In the field of geophysical fluid dynamics the interaction of coherent vortices is of significant interest, but further testing of the ellipsoidal moment model is required before the connection to interacting three dimensional vortices can be conclusively made. In order to further understand the process by which two vortices merge, it should be possible to create a Lagrangian explanation for three-dimensional vortex merger by looking at hyperbolic fixed points of the co-rotating flow induced by the vortices in the ellipsoidal moment model, as in two dimensions. This explanation could also be explored in the context of the numerically computed quasigeostrophic flows. Finally, higher-resolution simulations are of course desirable for further understanding, especially of the role of diffusive spreading in initiating vortex merger events.

ACKNOWLEDGMENTS

One of the authors (K.J.) acknowledges support from NSF Grant No. OCE-0137347 and a University of Colorado Faculty Fellowship Award. Two authors (N.M.-B. and M.R.P.) were supported by NSF VIGRE Grant No. DMS-9810751 and NSF Grant No. OCE-0137347.

APPENDIX: MOMENT MODEL DERIVATION

For an index $\boldsymbol{\mu}$, consider the following functionals of $q(x,y,z)$ called *moments*:

$$a^{\boldsymbol{\mu}} = \int_{\mathbb{R}^3} q m^{\boldsymbol{\mu}} \, \mathrm{d}\boldsymbol{x},$$

where $m^{\boldsymbol{\mu}}$ is some function. Considering a vector of moments $\boldsymbol{a}=(a^{\boldsymbol{\mu}})$, where $\boldsymbol{\mu}$ ranges over some set of indices, the noncanonical Poisson bracket for functionals that only depend on those moments $f=f(\boldsymbol{a}), g=g(\boldsymbol{a})$ is

$$\{f,g\} = \frac{\partial f}{\partial a^{\boldsymbol{\mu}}} J^{\boldsymbol{\mu\nu}} \frac{\partial g}{\partial a^{\boldsymbol{\nu}}}, \tag{A1}$$

where summation over repeated indices is implied. $J^{\boldsymbol{\mu\nu}}$ is the *cosymplectic form*

$$J^{\boldsymbol{\mu\nu}} = \int_{\mathbb{R}^3} q[m^{\boldsymbol{\mu}}, m^{\boldsymbol{\nu}}] \, \mathrm{d}\boldsymbol{x} = \sigma_{\boldsymbol{\rho}}^{\boldsymbol{\mu\nu}} a^{\boldsymbol{\rho}} \tag{A2}$$

and $\sigma_{\boldsymbol{\rho}}^{\boldsymbol{\mu\nu}}$ are called the *coupling coefficients* for the given set of moments. The closure of the second-order moments under the action of the Jacobian $[m^{\boldsymbol{\mu}}, m^{\boldsymbol{\nu}}] = \sigma_{\boldsymbol{\rho}}^{\boldsymbol{\mu\nu}} m^{\boldsymbol{\rho}}$ is crucial for our reduction. With this representation of the Poisson bracket, if we can find a functional $\widetilde{H}(\boldsymbol{a}) \approx H$, we can then construct a finite-dimensional Hamiltonian system

$$\frac{\partial a^{\boldsymbol{\mu}}}{\partial t} = \{a^{\boldsymbol{\mu}}, \widetilde{H}\} = J^{\boldsymbol{\mu\nu}} \frac{\partial \widetilde{H}}{\partial a^{\boldsymbol{\nu}}},$$

which approximates the infinite-dimensional system.

Using the above representation of the Poisson bracket, it can be seen that any quantity $C=C(\boldsymbol{a})$, where $\boldsymbol{\nabla}_{\boldsymbol{a}} C$ is a null vector of $J^{\boldsymbol{\mu\nu}}$, is a conserved quantity, because

$$\frac{\mathrm{d}C}{\mathrm{d}t} = \{C,H\} = \frac{\partial C}{\partial a^{\boldsymbol{\mu}}} J^{\boldsymbol{\mu\nu}} \frac{\partial H}{\partial a^{\boldsymbol{\nu}}} = 0.$$

These quantities (C) are the *Casimir invariants* for the Poisson bracket. The Casimirs do not depend on the specific Hamiltonian used since $\{C,f\}=0$ for any functional f.

1. Ellipsoidal vortices

For N disjoint regions $D_i, i=1,\ldots,N$ of nonzero potential vorticity, consider the $10N$ moments up to quadratic order

$$a_i^{\boldsymbol{\mu}} = \int_{D_i} q m^{\boldsymbol{\mu}} \, \mathrm{d}\boldsymbol{x}, \quad i = 1, \ldots, N, \tag{A3}$$

$$m^{\boldsymbol{\mu}} = x^{\xi} y^{\eta} z^{\zeta}, \quad \xi, \eta, \zeta \geqslant 0, \quad \xi + \eta + \zeta \leqslant 2, \tag{A4}$$

where $\boldsymbol{\mu}=(\xi,\eta,\zeta)$ is a multi-index. We will also use the multi-index as an exponent for position vectors, defining $\boldsymbol{x}^{\boldsymbol{\mu}} = x^{\xi} y^{\eta} z^{\zeta}$. This gives a compact representation of the moments $a_i^{\boldsymbol{\mu}} = \int_{D_i} q \boldsymbol{x}^{\boldsymbol{\mu}} \, \mathrm{d}\boldsymbol{x}$. Since the regions D_i and D_j are disjoint for $i \neq j$, the cosymplectic form (A2) splits into blocks $J=(J_i^{\boldsymbol{\mu\nu}})_{i=1}^N$, $J_i^{\boldsymbol{\mu\nu}} = \sigma_{\boldsymbol{\rho}}^{\boldsymbol{\mu\nu}} a_i^{\boldsymbol{\mu}}$. In addition, we can write the Hamiltonian as the sum of the self-energy of each region and the energy of the pairwise interactions of different regions:

$$H = \sum_{i=1}^{N} H^{(s)}(\boldsymbol{a}_i) + \sum_{\substack{i,j=1 \\ i<j}}^{N} H^{(p)}(\boldsymbol{a}_i, \boldsymbol{a}_j).$$

In the case of an ellipsoidal region D_i of constant potential vorticity q_i, the self-energy is given by an elliptic integral

$$\begin{aligned} H^{(s)}(\boldsymbol{a}_i) &= \frac{3}{40\pi} (a_i^{\boldsymbol{0}})^2 \int_0^{\infty} K_i(s) \, \mathrm{d}s, \\ K_i(s)^{-2} &= s^3 + p_i^{(2)} s^2 + p_i^{(1)} s + p_i^{(0)} \\ &= (s+\alpha_i^2)(s+\beta_i^2)(s+\gamma_i^2), \end{aligned} \tag{A5}$$

where $p_i^{(2)}, p_i^{(1)}, p_i^{(0)}$ are known functions of the six moments of second order, and α_i, β_i, and γ_i are the semi-axes of the ith ellipsoid.[14,44] The pairwise interaction Hamiltonian

$$H^{(p)}(\boldsymbol{a}_i, \boldsymbol{a}_j) = H_{ij}^{(p)} = \frac{1}{2} \left(\int_{D_i} q_i \psi_j \, \mathrm{d}\boldsymbol{x} + \int_{D_j} q_j \psi_i \, \mathrm{d}\boldsymbol{x} \right),$$

where q_i is the potential vorticity field in region D_i and ψ_i is the induced velocity field, must be approximated to be represented in terms of the second moments.

2. The pairwise interaction Hamiltonian

Our approximation of $H_{ij}^{(p)}$ in terms of the moments up to second order is an asymptotic expansion in the ratio of the vortex size and the vortex separation. We assume that this parameter is small and keep terms that are order 1. Instead of using the $10N$ moments specified before, more natural coordinates are the circulation $a_i^{\mathbf{0}}$, the centroids of the vortices $\boldsymbol{x}_i=(a_i^{1,0,0},a_i^{0,1,0},a_i^{0,0,1})/a_i^{\mathbf{0}}$ and the scaled and shifted second moments

$$c_i^{\boldsymbol{\mu}}=\frac{a_i^{\boldsymbol{\mu}}}{a_i^{\mathbf{0}}}-\boldsymbol{x}_i^{\boldsymbol{\mu}}=\frac{1}{a_i^{\mathbf{0}}}\int_{D_i}q(\boldsymbol{x}-\boldsymbol{x}_i)^{\boldsymbol{\mu}}\,\mathrm{d}\boldsymbol{x},\quad \alpha+\beta+\gamma=2.$$

We will use $\boldsymbol{b}_i=(a_i^{\mathbf{0}},\boldsymbol{x}_i,c_i^{\boldsymbol{\mu}})$ as the ten coordinates of each vortex. The only necessary change in the equations of motion is to replace $J^{\boldsymbol{\mu\nu}}$ by

$$\tilde{J}_i^{\boldsymbol{\mu\nu}}=\frac{\partial b_i^{\boldsymbol{\mu}}}{\partial a_i^{\boldsymbol{\rho}}}J_i^{\boldsymbol{\rho\kappa}}\frac{\partial b_i^{\boldsymbol{\kappa}}}{\partial a_i^{\boldsymbol{\nu}}}. \tag{A6}$$

Define $\boldsymbol{x}_{ij}=\boldsymbol{x}_i-\boldsymbol{x}_j$, $R_{ij}=|\boldsymbol{x}_{ij}|$ and $c_{ij}^{\boldsymbol{\mu}}=c_i^{\boldsymbol{\mu}}+c_j^{\boldsymbol{\mu}}$. Then, to first order in the (assumed) small parameter $\epsilon=c_i^{\boldsymbol{\mu}}/R_{ij}\ll 1$, the interaction Hamiltonian is

$$\begin{aligned}\tilde{H}_{ij}^{(p)}=\tilde{H}^{(p)}(\boldsymbol{b}_i,\boldsymbol{b}_j)=\frac{a_i^{\mathbf{0}}a_j^{\mathbf{0}}}{R_{ij}}\Bigg\{1&-\frac{1}{2R_{ij}^2}(c_{ij}^{2,0,0}+c_{ij}^{0,2,0}+c_{ij}^{0,0,2})\\&+\frac{3}{2R_{ij}^4}[x_{ij}^2c_{ij}^{2,0,0}+y_{ij}^2c_{ij}^{0,2,0}+z_{ij}^2c_{ij}^{0,0,2}\\&+2x_{ij}y_{ij}c_{ij}^{1,1,0}+2x_{ij}z_{ij}c_{ij}^{1,0,1}\\&+2y_{ij}z_{ij}c_{ij}^{0,1,1}]\Bigg\},\end{aligned} \tag{A7}$$

$$H_{ij}^{(p)}=\tilde{H}_{ij}^{(p)}+O(\epsilon).$$

[1] B. Fornberg, "A numerical study of 2D turbulence," J. Comput. Phys. **25**, 1 (1977).
[2] J. C. McWilliams, "The emergence of isolated coherent vortices in turbulent flow," J. Fluid Mech. **146**, 21 (1984).
[3] G. F. Carnevale, J. C. McWilliams, Y. Pomeau, J. B. Weiss, and W. R. Young, "Evolution of vortex statistics in two-dimensional turbulence," Phys. Rev. Lett. **66**, 2735 (1991).
[4] A. Provenzale, "Transport by coherent bartotropic vortices," Annu. Rev. Fluid Mech. **31**, 55 (1999).
[5] J. C. McWilliams, "Statistical properties of decaying geostrophic turbulence," J. Fluid Mech. **198**, 199 (1989).
[6] J. C. McWilliams, J. B. Weiss, and I. Yavneh, "Anisotropy and coherent vortex structures in planetary turbulence," Science **264**, 410 (1994).
[7] J. C. McWilliams, J. B. Weiss, and I. Yavneh, "The vortices of homogeneous geostrophic turbulence," J. Fluid Mech. **401**, 1 (1999).
[8] D. G. Dritschel, M. de la Torre Juárez, and M. H. P. Ambaum, "The three-dimensional vortical nature of atmospheric and oceanic turbulent flows," Phys. Fluids **11**, 1512 (1999).
[9] G. G. Sutyrin, J. C. McWilliams, and R. Saravanan, "Co-rotating stationary states and vertical alignment of geostrophic vortices with thin cores," J. Fluid Mech. **357**, 321 (1998).
[10] S. Kida, "Motion of an elliptic vortex in a uniform shear flow," J. Phys. Soc. Jpn. **50**, 3517 (1981).
[11] M. V. Melander, N. J. Zabusky, and A. S. Styczek, "A moment model for vortex interactions of the two-dimensional Euler equations. Part 1. Computational validation of a Hamiltonian elliptical representation," J. Fluid Mech. **167**, 95 (1986).
[12] J. B. Weiss and J. C. McWilliams, "Temporal scaling behavior of decaying two-dimensional turbulence," Phys. Fluids A **5**, 608 (1993).
[13] S. P. Meacham, K. K. Pankratov, A. F. Shchepetkin, and V. V. Zhmur, "The interaction of ellipsoidal vortices with background shear flows in a stratified fluid," Dyn. Atmos. Oceans **21**, 167 (1994).
[14] S. P. Meacham, P. J. Morrison, and G. R. Flierl, "Hamiltonian moment reduction for describing vortices in shear," Phys. Fluids **9**, 2310 (1997).
[15] T. Miyazaki, Y. Furuichi, and N. Takahashi, "Quasigeostrophic ellipsoidal vortex model," J. Phys. Soc. Jpn. **70**, 1942 (2001).
[16] J. N. Reinaud, D. G. Dritschel, and C. R. Koudella, "The shape of vortices in quasi-geostrophic turbulence," J. Fluid Mech. **474**, 175 (2003).
[17] J. von Hardenberg, J. C. McWilliams, A. Provenzale, A. Shchepetkin, and J. B. Weiss, "Vortex merging in quasi-geostrophic flows," J. Fluid Mech. **412**, 331 (2000).
[18] D. G. Dritschel, "Vortex merger in rotating stratified flows," J. Fluid Mech. **455**, 83 (2002).
[19] J. N. Reinaud and D. G. Dritschel, "The merger of vertically offset quasi-geostrophic vortices," J. Fluid Mech. **469**, 287 (2002).
[20] D. G. Dritschel, J. N. Reinaud, and W. J. McKiver, "The quasi-geostrophic ellipsoidal vortex model," J. Fluid Mech. **505**, 201 (2004).
[21] J. N. Reinaud and D. G. Dritschel, "The critical merger distance between two co-rotating quasi-geostrophic vortices," J. Fluid Mech. **522**, 357 (2005).
[22] J. Clyne, T. Scheitlin, and J. B. Weiss, "Volume visualizing high-resolution turbulence computations," Theor. Comput. Fluid Dyn. **11**, 195 (1998).
[23] P. D. Reasor and M. T. Montgomery, "Three-dimensional alignment and corotation of weak, TC-like vortices via linear vortex Rossby waves," J. Atmos. Sci. **59**, 2306 (2001).
[24] J. C. McWilliams, L. P. Graves, and M. T. Montgomery, "A formal theory for vortex Rossby waves and vortex evolution," Geophys. Astrophys. Fluid Dyn. **97**, 275 (2003).
[25] J. Pedlosky, *Geophysical Fluid Dynamics* (Springer-Verlag, New York, 1987).
[26] R. Salmon, *Lectures on Geophysical Fluid Dynamics* (Oxford University Press, Oxford, 1998).
[27] T. Miyazaki, A. Asai, M. Yamamoto, and S. Fujishima, "Numerical validation of quasigeostrophic ellipsoidal vortex model," J. Phys. Soc. Jpn. **71**, 2687 (2002).
[28] S. P. Meacham, "Quasigeostrophic, ellipsoidal vortices in a stratified fluid," Dyn. Atmos. Oceans **16**, 189 (1992).
[29] M. V. Melander, N. J. Zabusky, and J. C. McWilliams, "Symmetric vortex merger in two dimensions: causes and conditions," J. Fluid Mech. **195**, 303 (1988).
[30] D. G. Dritschel and D. W. Waugh, "Quantification of the inelastic interaction of unequal vortices in two-dimensional vortex dynamics," Phys. Fluids A **4**, 1737 (1992).
[31] R. W. Brankin, I. Gladwell, and L. F. Shampine, "RKSUITE: a suite of Runge-Kutta codes for the initial value problem for ODEs," Technical Report 92-S1, Department of Mathematics, Southern Methodist University, Dallas, TX (1992).
[32] R. Piessens, E. deDoncker Kapenga, C. Ueberhuber, and D. Kahaner, *Quadpack: a Subroutine Package for Automatic Integration*, Series in Computational Mathematics (Springer-Verlag, New York, 1983).
[33] A. Wolf, J. B. Swift, H. L. Swinney, and J. A. Vastano, "Determining Lyapunov exponents from a time series," Physica D **16**, 285 (1985).
[34] J.-P. Eckmann and D. Ruelle, "Ergodic theory of chaos and strange attractors," Rev. Mod. Phys. **57**, 617 (1985).
[35] G. A. Gottwald and I. Melbourne, "A new test for chaos in deterministic systems," Proc. R. Soc. London, Ser. A **460**, 603 (2004).
[36] D. G. Dritschel and M. de la Torre Juárez, "The instability and breakdown of tall columnar vortices in a quasi-geostrophic fluid," J. Fluid Mech. **328**, 129 (1996).
[37] J. C. McWilliams, "The vortices of two-dimensional turbulence," J. Fluid Mech. **219**, 261 (1990).
[38] T. B. Mitchell and C. F. Driscoll, "Electron vortex orbits and merger," Phys. Fluids **8**, 1828 (1996).
[39] M. Jentschel, A. Thess, and U. Bahr, "Lyapunov exponents and the merger of point-vortex clusters," Phys. Rev. E **51**, 5120 (1995).
[40] B. Fornberg, *A Practical Guide to Pseudospectral Methods* (Cambridge University Press, Cambridge, UK, 1998).
[41] J. P. Boyd, *Chebyshev and Fourier Spectral Methods* (Dover, New York, 2001).

[42]P. R. Spalart, R. D. Moser, and M. M. Rogers, "Spectral methods for the Navier-Stokes equations with one infinite and two periodic directions," J. Comput. Phys. **96**, 297 (1991).
[43]D. A. Schechter, M. T. Montgomery, and P. D. Reasor, "A theory for the vertical alignment of a quasigeostrophic vortex," J. Atmos. Sci. **59**, 150 (2002).
[44]S. Chandrasekhar, *Ellipsoidal Figures of Equilibrium* (Dover, New York, 1987).